ISSN 1007-9327 (print)
ISSN 2219-2840 (online)

World Journal of *Gastroenterology*

World J Gastroenterol 2023 August 7; 29(29): 4481-4603

Published by Baishideng Publishing Group Inc

World Journal of Gastroenterology

Contents

Weekly Volume 29 Number 29 August 7, 2023

REVIEW

ORIGINAL ARTICLE

Basic Study

Case Control Study

Retrospective Study

Observational Study

ABOUT COVER

Editorial Board Member of *World Journal of Gastroenterology*, Wan-Long Chuang, MD, PhD, Hepatobiliary Division, Department of Internal Medicine, Kaohsiung Medical University Hospital, Kaohsiung 807, Taiwan. waloch@kmu.edu.tw

AIMS AND SCOPE

The primary aim of *World Journal of Gastroenterology* (*WJG*, *World J Gastroenterol*) is to provide scholars and readers from various fields of gastroenterology and hepatology with a platform to publish high-quality basic and clinical research articles and communicate their research findings online. *WJG* mainly publishes articles reporting research results and findings obtained in the field of gastroenterology and hepatology and covering a wide range of topics including gastroenterology, hepatology, gastrointestinal endoscopy, gastrointestinal surgery, gastrointestinal oncology, and pediatric gastroenterology.

INDEXING/ABSTRACTING

The *WJG* is now abstracted and indexed in Science Citation Index Expanded (SCIE, also known as SciSearch®), Current Contents/Clinical Medicine, Journal Citation Reports, Index Medicus, MEDLINE, PubMed, PubMed Central, Scopus, Reference Citation Analysis, China National Knowledge Infrastructure, China Science and Technology Journal Database, and Superstar Journals Database. The 2023 edition of Journal Citation Reports® cites the 2022 impact factor (IF) for *WJG* as 4.3; IF without journal self cites: 4.1; 5-year IF: 5.3; Journal Citation Indicator: 0.82; Ranking: 33 among 93 journals in gastroenterology and hepatology; and Quartile category: Q2. The *WJG*'s CiteScore for 2021 is 8.3 and Scopus CiteScore rank 2022: Gastroenterology is 22/149.

RESPONSIBLE EDITORS FOR THIS ISSUE

Production Editor: *Hua-Ge Yu*; **Production Department Director:** *Xiang Li*; **Editorial Office Director:** *Jia-Ru Fan.*

NAME OF JOURNAL
World Journal of Gastroenterology

ISSN
ISSN 1007-9327 (print) ISSN 2219-2840 (online)

LAUNCH DATE
October 1, 1995

FREQUENCY
Weekly

EDITORS-IN-CHIEF
Andrzej S Tarnawski

EDITORIAL BOARD MEMBERS
http://www.wjgnet.com/1007-9327/editorialboard.htm

PUBLICATION DATE
August 7, 2023

INSTRUCTIONS TO AUTHORS
https://www.wjgnet.com/bpg/gerinfo/204

GUIDELINES FOR ETHICS DOCUMENTS
https://www.wjgnet.com/bpg/GerInfo/287

GUIDELINES FOR NON-NATIVE SPEAKERS OF ENGLISH
https://www.wjgnet.com/bpg/gerinfo/240

PUBLICATION ETHICS
https://www.wjgnet.com/bpg/GerInfo/288

PUBLICATION MISCONDUCT
https://www.wjgnet.com/bpg/gerinfo/208

ARTICLE PROCESSING CHARGE
https://www.wjgnet.com/bpg/gerinfo/242

STEPS FOR SUBMITTING MANUSCRIPTS
https://www.wjgnet.com/bpg/GerInfo/239

ONLINE SUBMISSION
https://www.f6publishing.com

World Journal of Gastroenterology

Submit a Manuscript: https://www.f6publishing.com

World J Gastroenterol 2023 August 7; 29(29): 4528-4541

DOI: 10.3748/wjg.v29.i29.4528

ISSN 1007-9327 (print) ISSN 2219-2840 (online)

ORIGINAL ARTICLE

Basic Study

Antagonizing adipose tissue-derived exosome miR-103-hepatocyte phosphatase and tensin homolog pathway alleviates autophagy in non-alcoholic steatohepatitis: A trans-cellular crosstalk

Miao-Miao Lu, Yue Ren, Yu-Wei Zhou, Ling-Ling Xu, Meng-Meng Zhang, Lin-Ping Ding, Wei-Xin Cheng, Xi Jin

Specialty type: Gastroenterology and hepatology

Provenance and peer review: Unsolicited article; Externally peer reviewed.

Peer-review model: Single blind

Peer-review report's scientific quality classification

Grade A (Excellent): 0
Grade B (Very good): B
Grade C (Good): C
Grade D (Fair): 0
Grade E (Poor): 0

P-Reviewer: Herrera B, Spain; Sukocheva OA, Australia

Received: April 5, 2023
Peer-review started: April 5, 2023
First decision: May 23, 2023
Revised: June 11, 2023
Accepted: July 4, 2023
Article in press: July 4, 2023
Published online: August 7, 2023

Miao-Miao Lu, Endoscopy Center, Children's Hospital of Zhejiang University School of Medicine, Hangzhou 310003, Zhejiang Province, China

Yue Ren, Yu-Wei Zhou, Lin-Ping Ding, Wei-Xin Cheng, Department of Medicine, Zhejiang University School of Medicine, Hangzhou 310003, Zhejiang Province, China

Ling-Ling Xu, Department of Gastroenterology, The Second People's Hospital of Yuhang District, Hangzhou 310003, Zhejiang Province, China

Meng-Meng Zhang, Department of Gastroenterology, Hangzhou Shangcheng District People's Hospital, Hangzhou 310003, Zhejiang Province, China

Xi Jin, Department of Gastroenterology, The First Affiliated Hospital of Zhejiang University School of Medicine, Hangzhou 310003, Zhejiang Province, China

Corresponding author: Xi Jin, MD, PhD, Doctor, Department of Gastroenterology, The First Affiliated Hospital of Zhejiang University School of Medicine, No. 79 Qingchun Road, Hangzhou 310003, Zhejiang Province, China. jxfl007@zju.edu.cn

Abstract

BACKGROUND

Obesity plays a vital role in the occurrence and development of non-alcoholic steatohepatitis (NASH). However, the underlining mechanism is still unclear, where adipose tissue (AT) derived exosomes may actively participate. MicroRNAs (miRNAs) are commonly secreted from exosomes for cell communication. Though the regulation of miR-103 on insulin sensitivity has been reported, the specific role of AT-derived exosomes miR-103 in NASH is still vague and further investigation may provide novel therapeutic choices.

AIM

To determine the specific role of AT-derived exosomes miR-103 in developing NASH through various methods.

METHODS

The expression levels of miR-103 in the AT-derived exosomes and livers were detected and compared between NASH mice and control. The effect of miR-103

on NASH progression was also explored by antagonizing miR-103, including steatosis and inflammation degree changes. The interaction between miR-103 and the autophagy-related gene phosphatase and tensin homolog (PTEN) was confirmed by dual-luciferase reporter assay. The role of the interaction between miR-103 and PTEN on autophagy was verified in NASH-like cells. Finally, the effects of miR-103 from adipose-derived exosomes on NASH and autophagy were analyzed through animal experiments.

RESULTS

The expression of miR-103 was increased in NASH mice, compared to the control, and inhibition of miR-103 could alleviate NASH. The results of the dual-luciferase reporter assay showed miR-103 could interact with PTEN. MiR-103-anta decreased p-AMPKa, p-mammalian target of rapamycin (mTOR), and p62 but increased the protein levels of PTEN and LC3-II/I and the number of autophagosomes in NASH mice. Similar results were also observed in NASH-like cells, and further experiments showed PTEN silencing inhibited the effect of miR-103-anta. AT derived-exosome miR-103 aggravated NASH and increased the expressions of p-AMPKa, p-mTOR, and p62 but decreased the protein levels of PTEN and LC3-II/I and the number of autophagosomes in mice.

CONCLUSION

AT derived-exosome increased the levels of miR-103 in the liver, and miR-103 aggravated NASH. Mechanically, miR-103 could interact with PTEN and inhibit autophagy.

Key Words: Non-alcoholic steatohepatitis; Nonalcoholic fatty liver disease; Exosomes; Phosphatase and tensin homolog

Core Tip: Our study confirms the important role of miR-103-phosphatase and tensin homolog-autophagy axis in the pathogenesis of non-alcoholic steatohepatitis (NASH). More importantly, the elevation of miR-103 in the liver of NASH mice is partly due to adipose tissue exosome secretion and integration, which also partially explains the mechanism of obesity leading to NASH.

Citation: Lu MM, Ren Y, Zhou YW, Xu LL, Zhang MM, Ding LP, Cheng WX, Jin X. Antagonizing adipose tissue-derived exosome miR-103-hepatocyte phosphatase and tensin homolog pathway alleviates autophagy in non-alcoholic steatohepatitis: A trans-cellular crosstalk. *World J Gastroenterol* 2023; 29(29): 4528-4541
URL: https://www.wjgnet.com/1007-9327/full/v29/i29/4528.htm
DOI: https://dx.doi.org/10.3748/wjg.v29.i29.4528

INTRODUCTION

Non-alcoholic fatty liver disease (NAFLD) is recognized as the hepatocellular manifestation of metabolic syndrome, characterized by hepatic lipid accumulation and inflammation, and precluded with secondary causes, such as chronic viral hepatitis, significant alcohol consumption, long-term use of steatogenic medication, and other chronic liver diseases including autoimmune hepatitis, hemochromatosis, Wilson's disease[1]. NAFLD is categorized into NAFL, non-alcoholic steatohepatitis (NASH), fibrosis, and even cirrhosis according to histological changes in different disease stages. Among them, NASH is considered the watershed in NAFLD and is defined as the presence of 5% hepatic steatosis and ensuing hepatocyte injury[1]. According to a previous meta-analysis, the pooled overall global prevalence of NAFLD was estimated to be 25.24% [95% confidence interval (CI): 22.10-28.65], while the pooled overall NASH prevalence among biopsied NAFLD patients was 59.10% (95%CI: 47.55-69.73)[2]. Moreover, fibrosis, which is closely related to liver cirrhosis, liver cancer, and other end-stage liver diseases, is more likely to occur in NASH patients than NAFL patients [3]. Those findings support the importance of NASH and suggest that the burden of disease caused by NASH needs to be paid adequate attention. NASH has become one of the leading causes of cirrhosis and the second leading cause of liver transplantation in the United States[4,5].

NAFLD is commonly associated with metabolic comorbidities such as obesity, diabetes mellitus, and dyslipidemia[2,6]. The prevalence of obesity is as high as 51.34% (95%CI: 41.38-61.20) and 81.83% (95%CI: 55.16-94.28) among NAFLD and NASH patients, respectively[2]. The effect of obesity on NAFLD has been intensively explored. On the one hand, the expansion of adipose tissue (AT) in obese people leads to increased circulating free fatty acids (FFAs) and leptin and decreased adiponectin, which leads to intrahepatic fat accumulation. On the other hand, the chronic inflammatory state caused by obesity will further lead to the infiltration of inflammatory cells in the liver, resulting in the progression of NAFLD[7]. Due to the important role of obesity in the occurrence and development of NAFLD, in-depth research on the mechanism of obesity leading to NASH may provide new therapeutic targets.

Exosomes are extracellular vesicles secreted by various cells and serve as an essential means of intercellular communication by delivering microRNAs (miRNAs), bioactive lipids, and regulatory proteins from one cell to another [8]. Previous studies have shown that AT-derived exosomes are essential in regulating insulin sensitivity[9,10], a common

manifestation of metabolic syndrome in patients with NAFLD. Previous studies have also shown that AT-derived exosome miRNAs are involved in the occurrence and development of various metabolic-related diseases[11]. Among them, miR-103 attracted our attention since previous studies have shown that miR-103 is involved in regulating insulin sensitivity[12]. The specific role of AT-derived exosomes in the development of NASH also deserves further study. Therefore, in this study, we focused on the specific role of AT-derived exosomes miR-103 in developing NASH through various methods.

MATERIALS AND METHODS

Ethics statement

This study followed the guidelines for the Care and Use of Laboratory Animals of the National Institute of Health. The animal protocol was approved by the institutional review board of the Tab of Animal Experimental Ethical Inspection of the First Affiliated Hospital of Zhejiang University. The Reference Number is 2020-1407.

The successful construction of NASH animal and cell models

C57BL/6 mice were routinely fed a high-fat diet for 12 wk to establish the NASH animal model. According to different treatments, they were initially divided into the control group (12% kcal fat, 66% kcal carbohydrate, 22% kcal protein) and the model group (60% kcal fat, 20% kcal carbohydrate, 20% kcal protein)[13]. Starting from the 13th wk, 40 mg/kg miR-negative control (NC)-anta and miR-103-anta were injected into the mice from the model group (dissolved in 0.2 mL normal saline) through the tail vein every 2 d thrice to construct miR-NC-anta model group and miR-103-anta model group. The control and model groups were injected with blank normal saline thrice (n = 10 in each group). Finally, the mice were sacrificed, where liver tissue, abdominal AT, and serum were collected and stored in a cryostorage tube at -80 °C for further analysis.

NASH-like cell model was constructed by conventional oleic acid (OA)-palmitic acid (PA) mixture culture (OA:PA = 2:1)[14]. Firstly, 128.2 mg PA (molecular weight: 256.42) was sequentially retrieved on a precision balance, 1 mL 1 M OA was added, vortex dissolved, and mixed in a small whirlpool, and then completely dissolved in a water bath at 55 °C-65 °C to obtain 1.5 M FFA mixture. After that, 1.5 M FFA with DMSO was dissolved into 0.1 M working solution. In the model group, Alpha mouse liver 12 (AML-12) cells were added with 400 μM FFA and cultured for 24 h, followed by transfection with miR-103-anta and its sh-phosphatase and tensin homolog (PTEN) and their relative controls. All further *in vitro* experiments were performed on those cells.

Exosome isolation and confirmation

Exosomes were extracted from the filtrate according to the manufacturer's instructions[15]. The diluted exosomes were subjected to NanoFCM (China) for transmission electron microscopy (TEM) and size distribution analysis for further confirmation.

Quantitative real-time polymerase chain reaction, ELISA, and western blotting

Total RNA was isolated using Trizol (Invitrogen, United States) and reverse-transcribed into cDNA using the First Strand cDNA Synthesis Kit (TransGen, China) following the manufacturer's instructions. Quantitative real-time polymerase chain reaction (qRT-PCR) was routinely performed using the SYBR Premix Ex Taq qPCR kit (TaKaRa, Japan). The alanine aminotransferase (ALT), aspartate aminotransferase (AST), total triglycerides (TG), total cholesterol (CHOL), superoxide dismutase (SOD), malondialdehyde (MDA), and H_2O_2 concentrations were detected using test kits according to the manufacturer's instructions. Total protein was isolated using radioimmune precipitation assay buffer (TaKaRa, Japan) supplemented with a protease inhibitor (Roche, Switzerland). After quantification using the BCA Protein Assay Kit (Thermo, United States), the proteins were separated by sodium-dodecyl sulfate gel electrophoresis and transferred onto polyvinylidene fluoride membranes. The membranes were blocked and incubated overnight with antibodies against PTEN (9188T, CST), p-AMPK (ab32047, Abcam), p-mammalian target of rapamycin (mTOR) (CSB-PA271384, Cusabio), LC3 (12741T, CST), p62 (ab91526, Abcam), and GAPDH (ab245355, Abcam) at 4 °C. The membranes were incubated with HRP-conjugated secondary antibodies (ab205718, Abcam). Finally, the protein bands were detected using enhanced chemiluminescence (ECL) kits (Thermo, United States).

Hematoxylin and eosin staining and oil red staining

The hematoxylin and eosin (HE) staining was performed using the HE staining kit (C0105S, Beyotime) according to the manufacturer's instructions. Oil red staining was performed using an oil red staining solution (G 1262, Solarbio; C0157S, Beyotime). Briefly, 5-10 μm thick fresh frozen tissue was placed on the slide and dried at room temperature for 30-60 min. The sections were fixed with 10% paraformaldehyde for 10 min, washed thrice with distilled water, and dried for several minutes. After that, the oil red was diluted with deionized water in a 3:2 ratio, with impurities removed by filter paper, and left for 10 min at room temperature. Preheated oil red was used for tissue dye in a 6 °C temperature box for 8-10 min. After the 85% propylene glycol solution was differentiated for 2-5 min, it was washed twice with distilled water and restained with hematoxylin for 30 s. After rinsing with running water for 3 min, the tablets can be sealed with glycerine gelatin.

Luciferase reporter assay and TEM

The luciferase reporter assay was performed according to the manufacturer's instructions of Pierce™ Cypridina-Firefly Luciferase Dual Assay Kit (16184, Thermo). Briefly, AML-12 cells were co-transfected with a 10 nM miR-103 or NC control, a 2 ng pRL-CMV, and a 20 ng firefly luciferase reporter plasmid containing PTEN of the wild-type or mutant 30-untranslated region. Then, 48 h after transfection, the cell lysates were determined by luciferase to observe the interaction between miR-103 and PTEN. The liver tissues with the size of 1 mm × 1 mm × 1 mm were fixed, dehydrated, impregnated, and embedded to make ultrathin sections (50-70 nm) and then stained with uranium acetate and lead citrate successively and dried for observation under TEM.

Immunofluorescence

The frozen slices of 5-10 μm thick liver tissue were dried at room temperature for 30-60 min. They were sequentially fixed with 10% paraformaldehyde for 10 min, rinsed thrice with distilled water, and dried for several minutes. After that, the antigen was repaired by microwave at 92 °C-96 °C for 10-15 min, cooled to room temperature naturally, and sealed with 5% BSA at 37 °C for 60 min. After pouring the excess serum, LC3-II/I antibody was diluted at 1:100, added into samples, and incubated at 4 °C overnight. Rinsed with phosphate buffered saline (PBS) the next day, samples were added to the mixture of the fluorescent secondary antibody and 4',6-diamidino-2-phenylindole at a ratio of 1:200 and incubated for 60 min at room temperature. After washing with PBS, laser confocal scanning for immunofluorescence was performed.

Transwell analysis

3T3-L1 cells were first routinely induced to differentiate into adipocytes to identify the transfer of miR-103 from adipocytes to AML-12 cells. After that, Cy3-labeled miR-103 was transfected and then co-cultured with the underlying AML-12 cells through a transwell chamber. AML-12 cells were then isolated, and immunofluorescence determined the red fluorescence value.

Cell transfection

Cells for transfection were incubated into a 6-well plate. 5-10 μL miR-NC-anta and miR-103-anta were absorbed and diluted into 250 μL Opti-MEMI reduced serum medium, mixed gently, and incubated at room temperature for 5 min. Then, 3-6 μL Lipofectamine® 2000 Reagent was diluted to 250 μL of Opti-MempI reduced-serum medium, lightly mixed, and incubated at room temperature for 5 min. Diluted miR-NC-anta, miR-103-anta, and diluted Lipofectamine® 2000 Reagent were carefully mixed, gently blended, and incubated at room temperature for 20 min to form the reagent complex. After that, cells were washed with 2 mL serum-free medium, added with 2 mL of Opti-MEMI low serum medium to each well, and then added to 500 μL of miR-NC-anta and miR-103-anta-Lipofectamine® 2000 Reagent complex. These reagents were gently mixed and prepared for use.

Statistical analysis

All data are presented as mean ± SD. Differences between the two groups were analyzed using the student's *t*-test for categorical data and the chi-square method for numerical data. All statistical analyses were performed using GraphPad 9.0.2 software. Statistical significance between groups was set at $P < 0.05$.

RESULTS

The expression of miR-103 was increased in NASH mice, and inhibition of miR-103 could alleviate NASH

First, we successfully constructed animal models of NASH. Compared with the control, ALT, AST, TG, and CHOL were increased in NASH mice (Figure 1A). Hepatocyte ballooning, inflammatory cell infiltration, and hepatic lipid accumulation were observed in the livers of NASH mice (Figures 1B and C). Furthermore, we successfully extracted and confirmed AT-derived and circulating exosomes (Supplementary Figure 1). Subsequently, the expression of miR-103 in the livers, AT-derived exosomes, and circulating exosomes was detected by qRT-PCR. MiR-103 expression levels in the livers, AT-derived exosomes, and circulating exosomes were significantly increased in the NASH model group compared with the control group. Antagonizing miR-103 decreased miR-103 expression in NASH mice, but miR-NC-anta had no significant effect in NASH mice (Figure 1D). In addition, compared with miR-NC-anta and the model group, miR-103-anta treatment significantly reduced serum ALT and AST, decreased serum CHOL and TG, and alleviated oxidative stress (Figure 1A). Histologically, HE and oil red staining of the liver also indicated that inhibition of miR-103 alleviated hepatocyte ballooning, inflammatory cell infiltration, and hepatic lipid accumulation. (Figures 1B and C). Our above results indicate that the miR-103 level is elevated in NASH model mice, and reducing the expression of miR-103 can alleviate NASH, suggesting the potential involvement of miR-103.

The interaction between miR-103 and PTEN is involved in the process of autophagy

To further investigate the regulatory mechanism of miR-103 on NASH, we used *TargetScan* to predict its downstream targets[16]. The predicted results showed that PTEN, a gene that plays an essential role in autophagy, might interact with miR-103. Therefore, we used a dual-luciferase reporting experiment to further confirm their interaction (Figure 2A). The wild-type PTEN could interact with miR-103, while the mutant PTEN could not. Next, the protein content of PTEN and autophagy-related proteins such as p-AMPKa, p-mTOR, LC3-II/I, and p62 were determined by western blot. The results showed that compared with the control group, the expressions of p-AMPKa, p-mTOR, and p62 were significantly

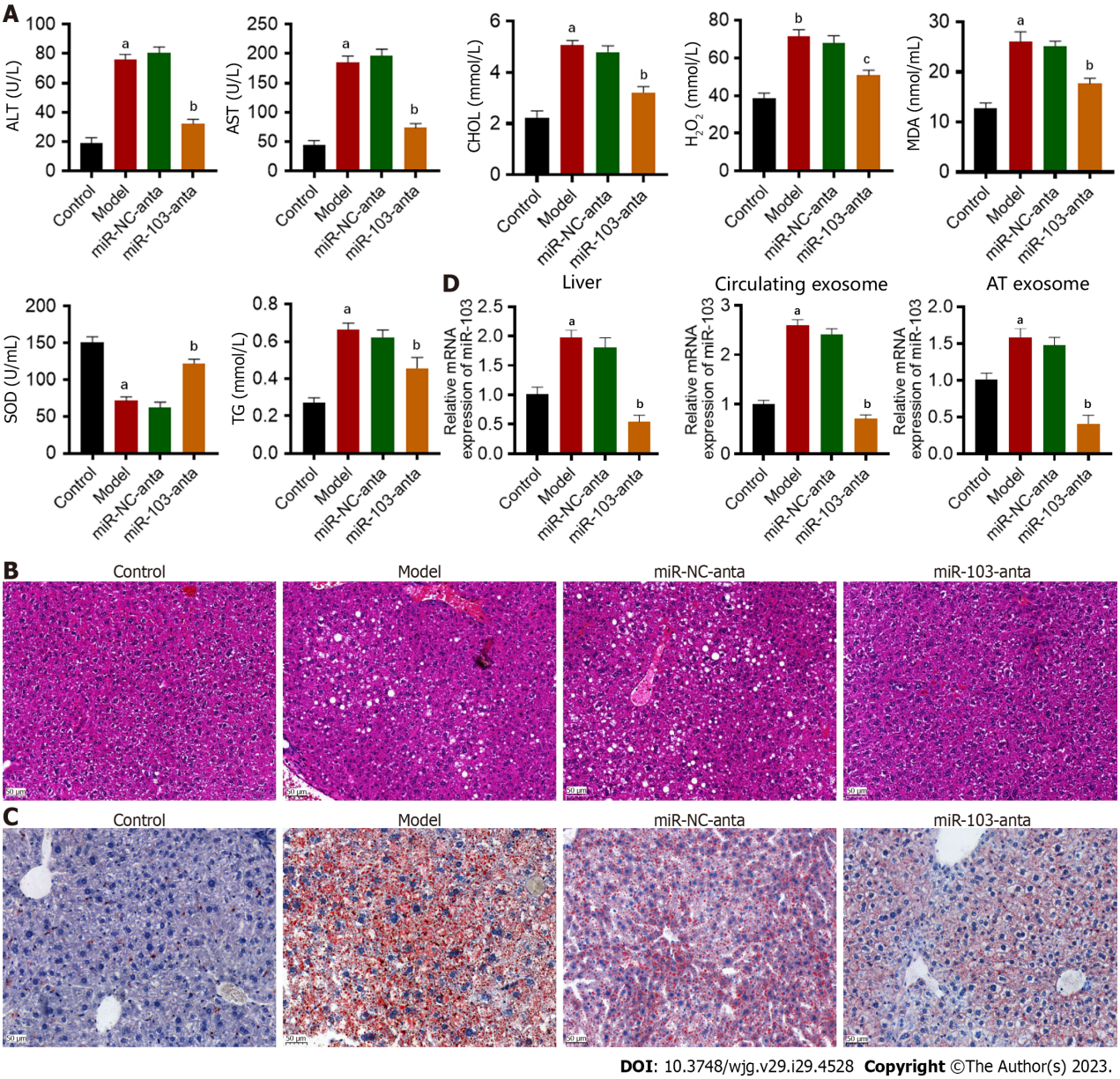

DOI: 10.3748/wjg.v29.i29.4528

Figure 1 The effect of miR-103 on the development of non-alcoholic steatohepatitis in mice. A: The results of ELISA to measure serum alanine aminotransferase (ALT), aspartate aminotransferase, total triglycerides, total cholesterol, superoxide dismutase, malondialdehyde, and H_2O_2; B: Hematoxylin and eosin staining of mice liver from different groups; C: Oil-red staining of mice liver from different groups; D: The expression of miR-103 in the liver, circulating exosomes, and adipose tissue-derived exosomes. $^{a}P < 0.01$ *vs* control; $^{b}P < 0.01$ *vs* model. ALT: Alanine aminotransferase; AST: Aspartate aminotransferase; TG: Total triglycerides; CHOL: Cholesterol; SOD: Superoxide dismutase; MDA: Malondialdehyde.

increased in the model group, while the protein levels of PTEN and LC3-II/I were decreased (Figure 2B). In addition, TEM and immunofluorescence staining showed that the number of autophagosomes in the liver of NASH model mice was significantly reduced compared with control mice (Figures 2C and D). However, compared with the model and miR-NC-anta groups, p-AMPKa, p-mTOR, p62, and the number of autophagosomes were significantly decreased in the miR-103-anta group. Similarly, the protein levels of PTEN and LC3-II/I was increased (Figures 2C and D). All these results indicate that autophagy is inhibited in the development of NASH, while miR-103-anta treatment could antagonize those changes. These results indicate that miR-103 interacts with PTEN and interferes with the downstream autophagy process, suggesting that the inhibition of autophagy in NASH may be attributed to the increased expression of miR-103.

MiR-103 participates in the development of NASH by inhibiting autophagy via interacting with PTEN

We then conducted *in vitro* experiments to further confirm our hypothesis. The results showed that inhibition of miR-103 expression could reduce the accumulation of lipids in NASH model cells, decrease the release of ALT and AST, and relieve oxidative stress. However, the effect of miR-103-anta was partially eliminated by silencing PTEN (Figures 3A and B). The above results indicate that miR-103 is involved in NASH formation partially through its interaction with PTEN. In addition, we detected the expression of autophagy-related proteins. We found that the expression of p-AMPKa, p-mTOR, and p62 was increased in NASH cells, while the expression of PTEN and LC3-II/I was decreased. Treatment with miR-

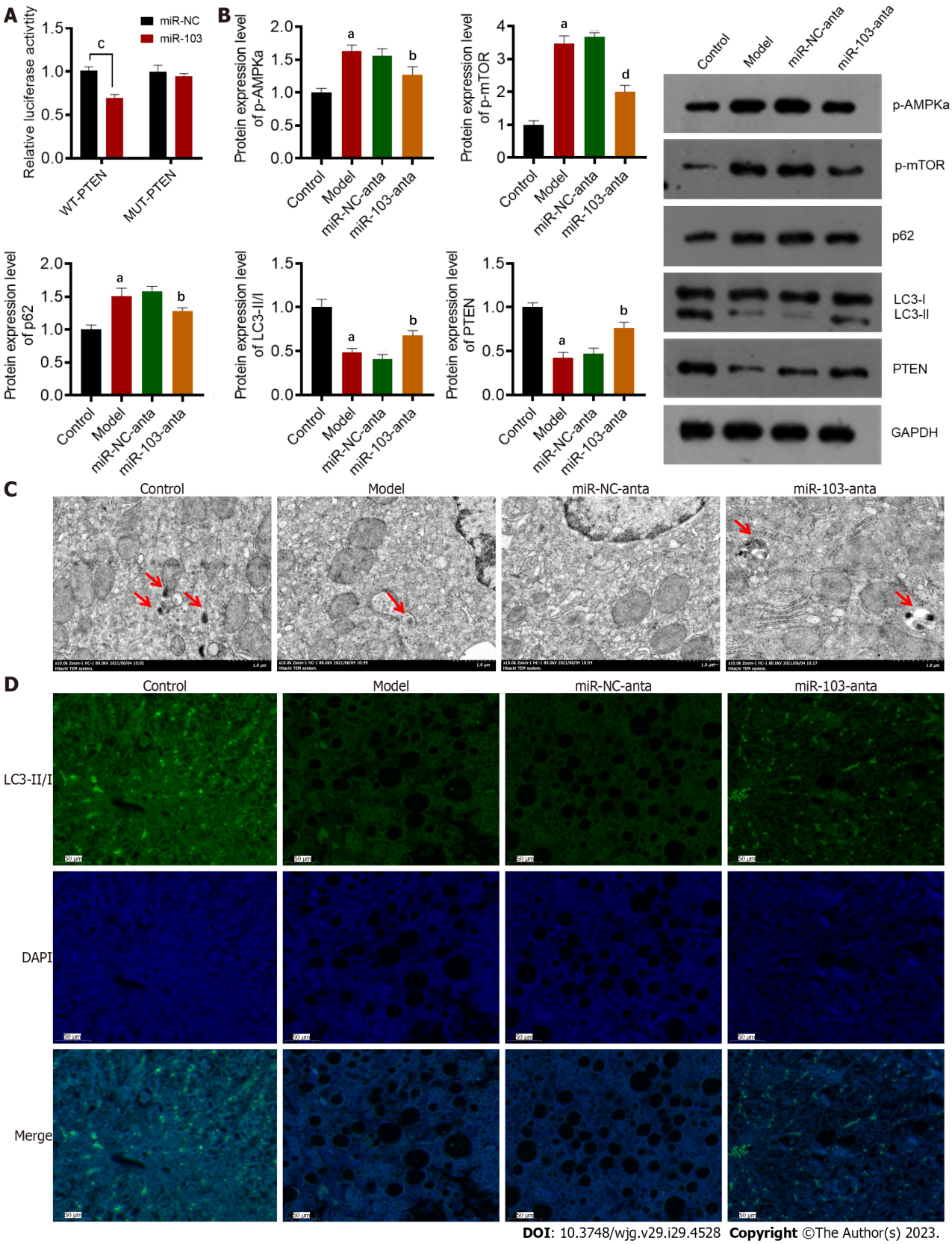

DOI: 10.3748/wjg.v29.i29.4528

Figure 2 The capacity of miR-103 in targeting phosphatase and tensin homolog gene and affecting autophagy. A: The luciferase reporter assay results verified the interaction between miR-103 and phosphatase and tensin homolog; B: Western blotting showed the differential expression of the autophagy-related protein; C: Transmission electron microscopy images of autophagosomes (red arrowhead) in the liver; D: The results of immunofluorescence staining showed liver autophagosomes in different groups. $^{a}P < 0.01$ *vs* control; $^{b}P < 0.01$ *vs* model; $^{c}P < 0.01$ *vs* miR-103; $^{d}P < 0.05$ *vs* model. PTEN: Phosphatase and tensin homolog; WT: Wild type; MUT: Mutant; DAPI: 4',6-diamidino-2-phenylindole; mTOR: Mammalian target of rapamycin; NC: Negative control.

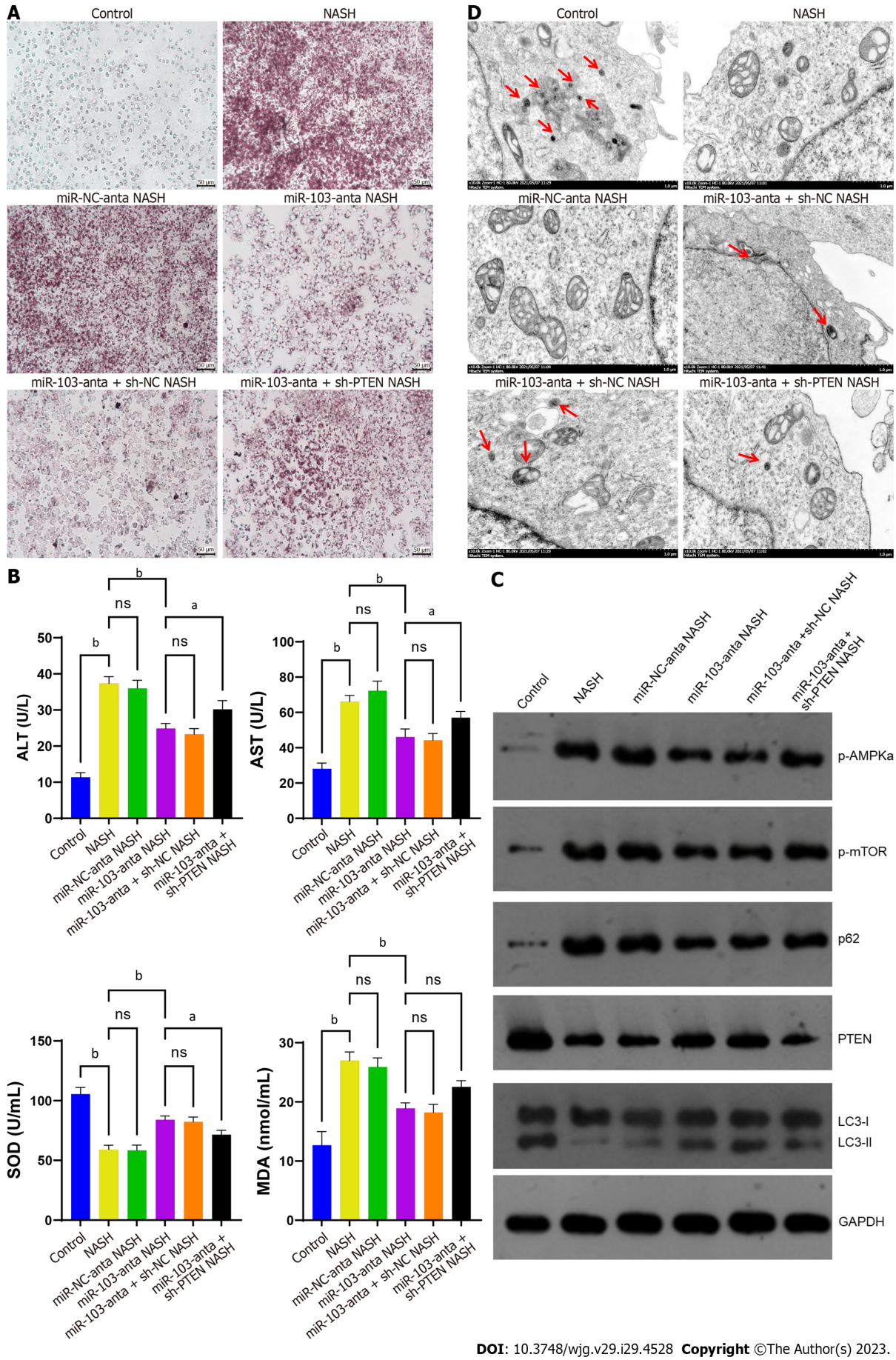

DOI: 10.3748/wjg.v29.i29.4528

Figure 3 *In vitro* experiments confirmed the interaction between miR-103 and phosphatase and tensin homolog gene. A: Oil-red staining of

cells from different groups showed different lipid droplet accumulation and inflammatory cell infiltration; B: The results of ELISA to measure serum alanine aminotransferase, aspartate aminotransferase, superoxide dismutase and malondialdehyde; C: Western blotting detected the expression of the autophagy-related protein of cells from different groups; D: Transmission electron microscopy pictures of autophagosomes (red arrowhead) in cells from different groups. $^{a}P < 0.05$, $^{b}P < 0.01$, ns: No significance. NASH: Non-alcoholic steatohepatitis; PTEN: Phosphatase and tensin homolog; NC: Negative control; ALT: Alanine aminotransferase; AST: Aspartate aminotransferase; TG: Total triglycerides; CHOL: Cholesterol; SOD: Superoxide dismutase; MDA: Malondialdehyde.

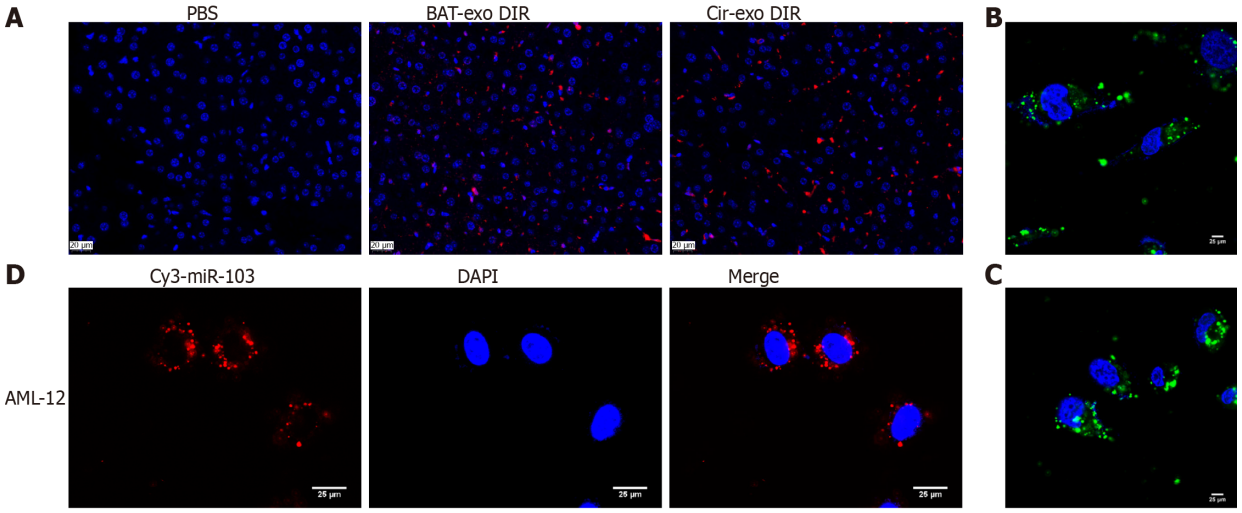

DOI: 10.3748/wjg.v29.i29.4528

Figure 4 MiR-103 transfers from adipocytes to hepatocytes. A: The fluorescence of liver tissue of mice injected with adipose tissue (AT)-exosomes or phosphate buffered saline; B: AT exosomes can be absorbed into alpha mouse liver 12 (AML-12) cells; C: Circulating exosomes can be absorbed into AML-12 cells; D: Transewell assay confirmed that miR-103 could be transferred from adipocytes to AML-12 cells. BAT: Brown adipose tissue; Exo: Exosomes; DIR: 1,1-dioctadecyl-3,3,3,3-tetramethylindotricarbocyaine iodide; Cir: Circulating; PBS: Phosphate buffered saline; DAPI: 4',6-diamidino-2-phenylindole; AML-12: Alpha mouse liver 12.

103-anta elevated the expression of PTEN and LC3-II/I and reduced the expression of p-AMPKa, p-mTOR, and p62 in NASH cells, while PTEN silencing inhibited the effect of miR-103-anta (Figure 3C). Finally, we also found that the number of autophagosomes decreased in NASH cells, and such declination was partially antagonized after the inhibition of miR-103. Similarly, PTEN silencing inhibited the effect of miR-103-anta (Figure 3D). To sum up, we confirmed the role of the miR-103-PTEN-autophagy axis in NASH through *in vitro* experiments.

Hepatocyte absorption of AT-derived exosome miR-103

To confirm that AT-derived exosomes can encapsulate miR-103 and target the liver, we conducted *in vivo* and *in vitro* experiments. In the *in vivo* experiment, AT and circulating exosomes of mice were extracted. The exo-DIR complex collected by centrifugation was injected into the tail vein of mice, and the PBS group was used as a control. The fluorescence of liver tissue was observed after mice scarification. There was no fluorescence in the PBS group but observed in AT-exo-DIR and cir-exo-DIR groups, with similar fluorescence intensity (Figure 4A). In the part of the *in vitro* experiment, the AT exosomes and circulating exosomes were detected by the FISH probe to migrate into AML-12 cells (Figures 4B and C). Further transewell assay showed that Cy3-labeled miR-103 could be transferred from adipocytes to AML-12 cells (Figure 4D).

Role of AT-derived exosome miR-103 in NASH

To verify the role of AT-derived exosome miR-103 in NASH through *in vivo* experiments, we extracted exosomes from mouse AT. We injected the extracted exosomes without other treatments and with miR-103-anta or miR-NC-anta into mice through the tail vein. Firstly, we found that injection of AT-derived exosomes increased the level of miR-103 in the liver, serum, and AT compared with the control group (Figure 5A). In addition, compared with the control group, treating AT-derived exosomes can increase serum ALT, AST, CHOL, and TG levels and aggravate oxidative stress (Figure 5B). Histologically, HE and oil red staining of the liver showed that treating AT-derived exosomes could aggravate hepatocyte ballooning, inflammatory cell infiltration, and intrahepatic lipid accumulation (Figures 5C and D). However, miR-103-anta treatment could partially eliminate such an effect while miR-NC-anta treatment could not, suggesting that AT-derived exosome aggravates NASH, and this effect is partly dependent on its encapsulated miR-103.

AT derived-exosome miR-103 inhibits autophagy in hepatocytes

To further verify *in vivo* that miR-103 in AT-derived exosomes is involved in NASH formation by influencing autophagy, we detected the expression of autophagy-related proteins in the liver of mice in each group. We found that compared with the control group, the expression of p-AMPKa, p-mTOR, and p62 in the livers of AT exosome-treated group was increased, while the expression of PTEN and LC3-II/I was decreased. Further miR-103-anta treatment increased the

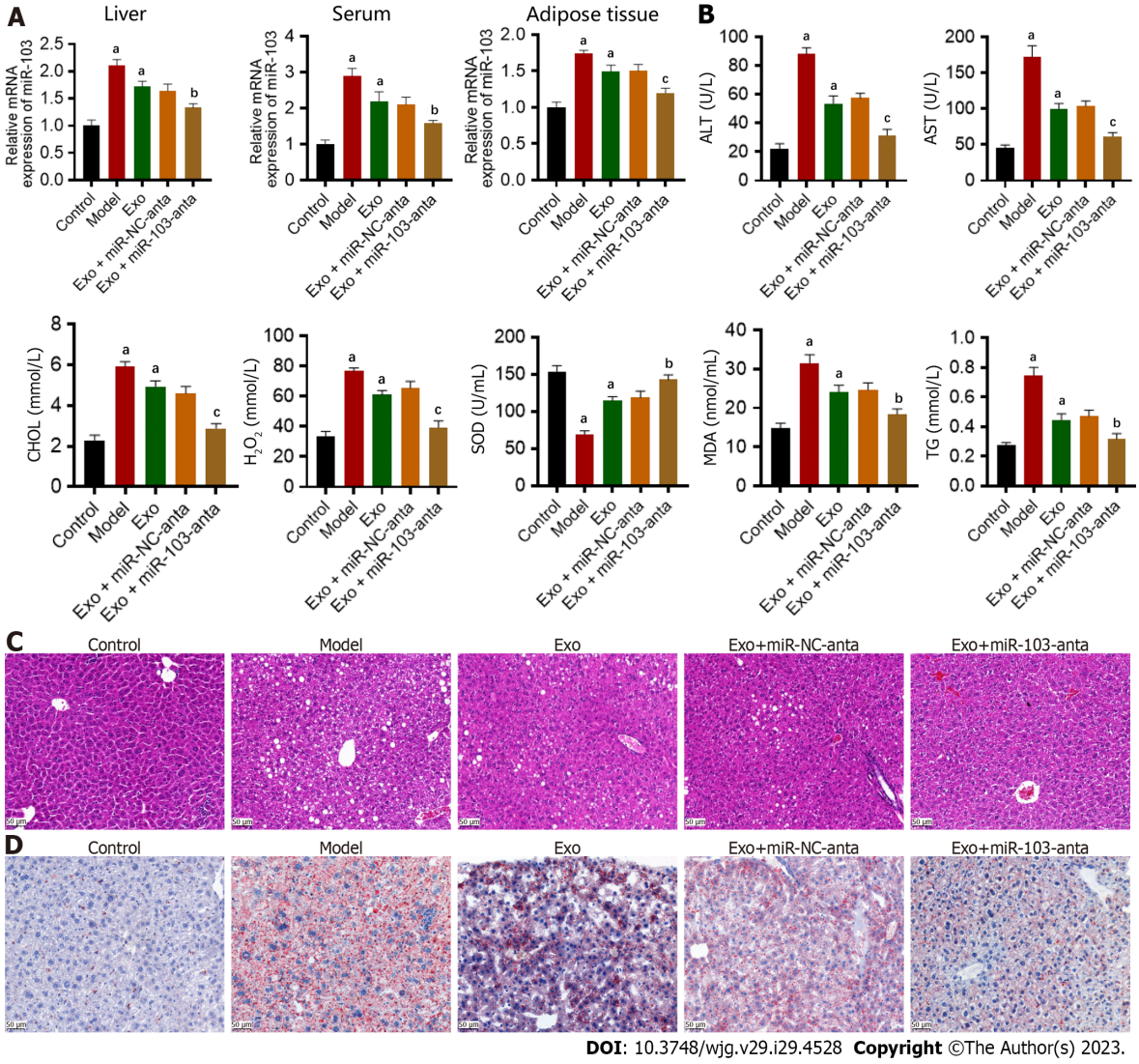

DOI: 10.3748/wjg.v29.i29.4528

Figure 5 The effect of adipose tissue-derived exosomes miR-103 on the development of non-alcoholic steatohepatitis in mice. A: The expression of miR-103 in the liver, serum, and adipose tissue; B: The results of ELISA to measure serum alanine aminotransferase, aspartate aminotransferase, total triglycerides, total cholesterol, superoxide dismutase, malondialdehyde, and H_2O_2; C: Hematoxylin and eosin staining of mice liver from different groups; D: Oil-red staining of mice liver from different groups. $^{a}P < 0.01$ *vs* control; $^{b}P < 0.05$ *vs* exosomes; $^{c}P < 0.01$ *vs* exosomes. Exo: Exosomes; NC: Negative control; ALT: Alanine aminotransferase; AST: Aspartate aminotransferase; TG: Total triglycerides; CHOL: Cholesterol; SOD: Superoxide dismutase; MDA: Malondialdehyde.

expression level of PTEN and LC3-II/I and reduced the expression level of p-AMPKa, p-mTOR, and p62, while miR-NC-anta had no similar effect (Figures 6A and B). Finally, through TEM and immunofluorescence, we found that the number of autophagosomes in the livers of mice treated with AT-derived exosomes was decreased, while miR-103-anta could partially antagonize such effect (Figures 6C and D).

DISCUSSION

NASH is considered the watershed in the progress of NAFLD, which is more closely related to the occurrence of liver cirrhosis and other complications. The prevalence of NASH has been increasing in recent years, resulting in a big challenge in disease burden and patient suffering. For instance, the lifetime cost of care for patients with NASH was around US $222 billion in 2017 in the United States[17]. More intriguingly, many NASH patients are obese and tend to have higher healthcare costs than non-obese NASH patients[18], but the etiology is still vague. Therefore, it is necessary to study the role and underlying mechanisms of obesity on NASH and further provide possible therapeutic targets. In this study, we confirmed the important role of AT-derived exosomes miR-103 in NASH and preliminary revealed its regulation on hepatocyte autophagy through targeting PTEN, which might partially provide the mechanisms by which obesity affects NASH.

MiRNA belongs to the family of non-coding RNA, which generally consists of 22 nucleotides[19] and regulates the mRNA levels of target genes[20]. Previous studies have identified a variety of miRNAs involved in metabolism-related diseases[21]. For example, miR-200 and miR-29 families play an important role in maintaining the balance between the

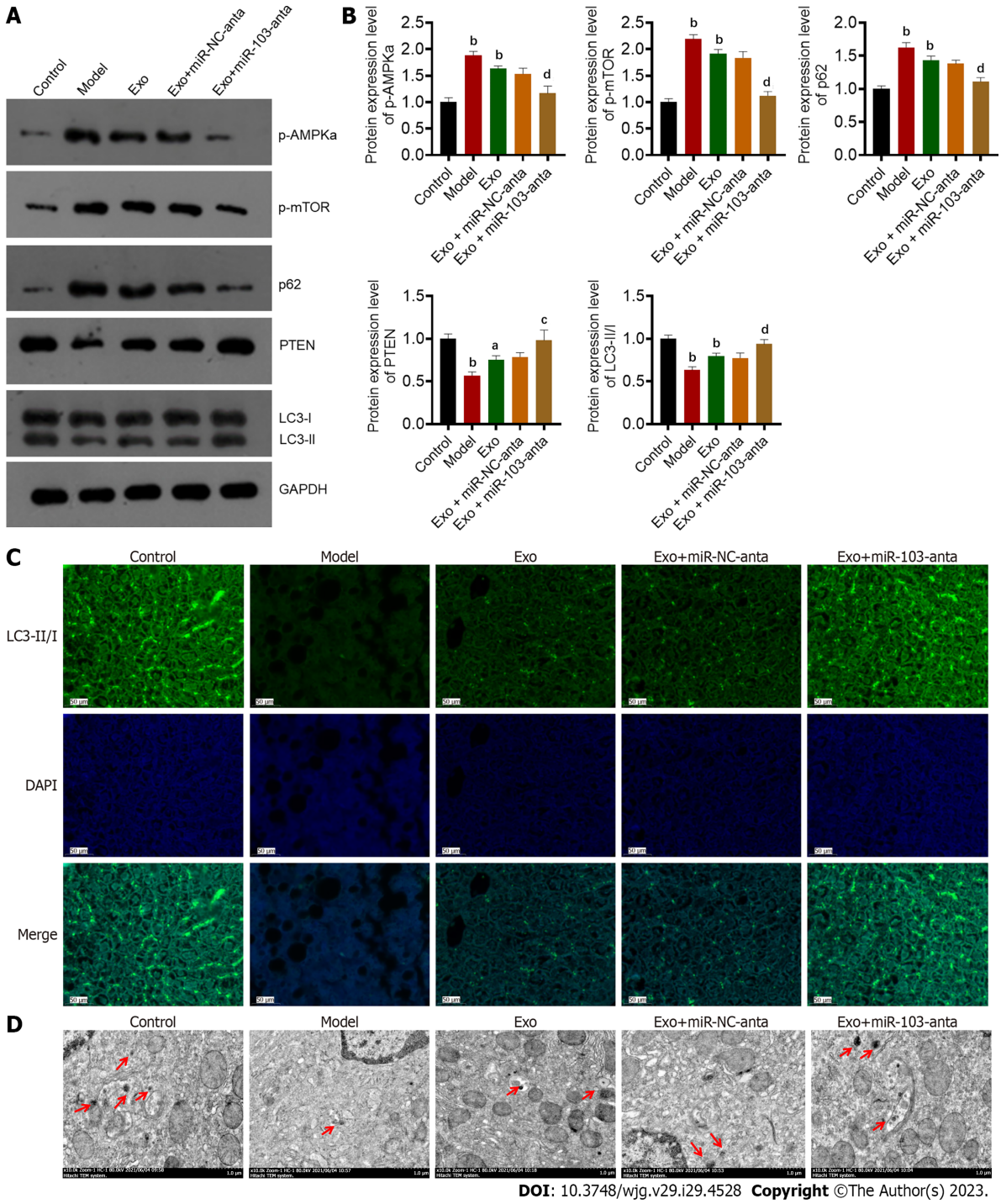

Figure 6 The effect of adipose tissue-derived exosomes miR-103 on autophagy in mice. A and B: Western blotting detected the expression of the autophagy-related protein; C: The results of immunofluorescence staining to observe autophagosomes in the liver from different groups; D: Transmission electron microscopy images of autophagosomes (red arrowhead) in the liver from different groups. $^{a}P < 0.05$ *vs* control; $^{b}P < 0.01$ *vs* control; $^{c}P < 0.05$ *vs* exosomes; $^{d}P < 0.01$ *vs* exosomes. Exo: Exosomes; PTEN: Phosphatase and tensin homolog; DAPI: 4',6-diamidino-2-phenylindole; mTOR: Mammalian target of rapamycin; NC: Negative control.

proliferation and differentiation of pancreatic β cells[22,23]. MiR-33a and miR-33b are involved in cholesterol and lipid metabolism[24,25]. Furthermore, several miRNAs are also targeting the liver to regulate metabolic processes. For instance, miR-122, one of the most abundant miRNAs in the liver, is involved in hepatic cholesterol and lipid metabolism [26,27]. Besides, miR-103, the focus of our study, has also been confirmed to be closely related to hepatic insulin sensitivity and the regulation of glucose homeostasis in previous studies[12]. Since NAFLD is the hepatic manifestation of metabolic syndrome, it is theoretically possible that miR-103 participates in NAFLD, but related research is still lacking. NASH was linked to menopause[28], and miR-103 was found to be linked to G protein-coupled estrogen receptor 1[29]. Therefore, the estrogen signaling pathway is the potential mechanism where miR-103 promotes NASH. However, in this study, for the first time, we showed that the miR-103 level in the liver of NASH mice was significantly increased while inhibiting miR-103 expression could alleviate NASH, suggesting that miR-103 is one of the potential targets for NASH

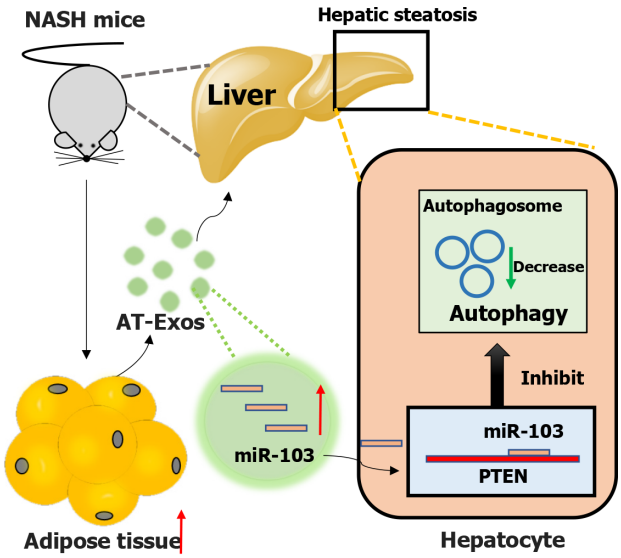

DOI: 10.3748/wjg.v29.i29.4528

Figure 7 The hypothesis of obesity-induced non-alcoholic steatohepatitis. The increased adipocyte tissue will secret more adipose tissue (AT)-derived exosomes, which include various contents, and miR-103 is our focus. The increased AT-derived exosomes miR-103 could be absorbed by hepatocytes and further regulate non-alcoholic steatohepatitis progression by affecting the autophagy process by targeting phosphatase and tensin homolog gene. AT: Adipose tissue; NASH: Non-alcoholic steatohepatitis; Exo: Exosomes; PTEN: Phosphatase and tensin homolog.

treatment.

We further identified the AT-derived exosomes as the source of miR-103 upregulation in the NASH mouse model. There have been many studies on the role of AT-derived exosomes in the development of NAFLD in obese people[30]. For instance, Fuchs *et al*[31] showed that the concentration of free exosomes is significantly higher in obese with NAFLD (OB-NAFLD) patients compared with lean with normal intrahepatic triglyceride content (LEAN) and obese with normal intrahepatic triglyceride content (OB-NL) populations and that these exosomes are at least partially derived from AT. Compared with exosomes derived from the LEAN and OB-NL groups, plasma and AT-derived exosomes from the OB-NAFLD group caused insulin resistance in both myotubes and hepatocytes, demonstrated by impaired insulin signaling. However, the underlying mechanism of the above effects of AT-derived exosomes in NAFLD patients has not been further explored. Our results complement this by revealing the effect of AT-derived exosomes through the miR-103-PTEN pathway, which broadens our understanding of NASH pathogenesis from the angle of trans-cellular crosstalk.

We also confirmed that autophagy is the downstream of the action of miR-103 through *in vivo* and *in vitro* experiments. Autophagy is an evolutionarily conserved cellular degradation process that delivers some intracellular components to lysosomes for degradation[32]. Current studies suggest that autophagy includes three subtypes: Macroautophagy, microautophagy, and chaperon-mediated autophagy[33]. Autophagy plays a vital role in the liver. It involves many basic liver functions, such as glycogenolysis, gluconeogenesis, and β-oxidation[34]. Previous studies have also shown that autophagy is hampered in NAFLD patients. Our previous study also revealed that autophagy inhibition plays an important role in NASH development[35]. Furthermore, restoring autophagy through certain drugs (trehalose, rapamycin, carbamazepine, or other pharmaceutical agents) or gene targets (overexpression of Atg7 or TFEB) can also alleviate NAFLD[36]. In addition, thyroxine[37] and caffeine[38] were also identified to reduce NAFLD by regulating liver autophagy. Therefore, miR-103 is expected to be one of the therapeutic targets for its autophagy regulation capacity and needs further clinical investigation in the future.

Some limitations in this study should be acknowledged. Firstly, AT-derived exosomes contain many non-coding RNAs, and we did not detect changes in the expression of other non-coding RNAs. Moreover, inhibition of miR-103 only partially inhibited the effect of AT-derived exosomes. Therefore, the above results suggest that AT-derived exosomes promote the development of NASH in multiple ways, and miR-103 is only one of them. Further research is needed on other reasons why AT-derived exosomes promote the development of NASH. Secondly, we did not design *in vivo* experiments to verify whether inhibition of autophagy could abolish the role of miR-103 in NASH. Therefore, in future studies, we may improve this part of the experiment and further explore the mechanism of miR-103 affecting autophagy. Finally, the preliminary data on the hepatocyte absorption of AT-derived exosome miR-103 needs further verification.

CONCLUSION

To sum up, our study confirms the important role of miR-103-PTEN - autophagy axis in NASH, and the elevation of miR-103 in the liver of the NASH model is partly due to hepatocyte absorption of AT derived-exosomes, which also partially explains the underlining mechanism of obesity leading to NASH (Figure 7).

ARTICLE HIGHLIGHTS

Research background

Non-alcoholic steatohepatitis (NASH) has become one of the leading causes of cirrhosis and the second leading cause of liver transplantation. miR-103 is involved in regulating insulin sensitivity, a common manifestation of metabolic syndrome in patients with NASH.

Research motivation

The specific role of miR-103 in the development of NASH also deserves further study.

Research objectives

To explore the specific role of miR-103 in the development of NASH and provide new therapeutic targets for NASH.

Research methods

The expression levels of miR-103 were detected and compared between NASH mice and control. The effect of miR-103 on NASH progression was explored by miR-103 antagonizing, including both changes of steatosis and inflammation degree. The interaction between miR-103 and the autophagy-related gene phosphatase and tensin homolog (PTEN) was confirmed by dual-luciferase reporter assay. The role of the interaction between miR-103 and PTEN on autophagy was verified in NASH cells. Finally, the effects of miR-103 from adipose tissue (AT)-derived exosomes on NASH and autophagy were analyzed through animal experiments.

Research results

The expression of miR-103 was increased in NASH mice, compared with the control, and inhibition of miR-103 could alleviate NASH. MiR-103 could interact with PTEN. MiR-103-anta inhibited autophagy in NASH mice. Further experiments showed PTEN silencing inhibited the effect of miR-103-anta. AT-derived exosome miR-103 aggravated NASH and inhibited autophagy in mice.

Research conclusions

AT derived-exosome increased the levels of miR-103 in the liver, and miR-103 aggravated NASH. Mechanically speaking, miR-103 could interact with PTEN and inhibit autophagy.

Research perspectives

MiR-103 may be a potential target for NASH treatment in the future.

FOOTNOTES

Author contributions: Jin X designed the report; Lu MM performed experiments, wrote the paper and assisted to design the report; Ren Y and Zhou YW performed experiments and statistical analysis; Zhang MM, Ding LP, and Cheng WX assisted to perform experiments and analyzed data; and all authors had access to the study data and reviewed and approved the final manuscript.

Supported by the Natural Science Foundation of Zhejiang Province, No. LZ21H030002.

Institutional animal care and use committee statement: This study was carried out following the recommendations in the Guide for the Care and Use of Laboratory Animals of the National Institute of Health. The animal protocol was approved by the institutional review board of the Tab of Animal Experimental Ethical Inspection of the First Affiliated Hospital of Zhejiang University. The Reference Number is 2020-1407.

Conflict-of-interest statement: All the authors report no relevant conflicts of interest for this article.

Data sharing statement: All the data included in this study are available upon request by contact with the corresponding author.

ARRIVE guidelines statement: The authors have read the ARRIVE guidelines, and the manuscript was prepared and revised according to the ARRIVE guidelines.

Country/Territory of origin: China

ORCID number: Miao-Miao Lu 0000-0002-9328-8239; Yue Ren 0000-0001-9071-2738; Ling-Ling Xu 0000-0002-6668-3057; Wei-Xin Cheng 0000-0003-1764-0779; Xi Jin 0000-0002-2975-977X.

S-Editor: Wang JJ
L-Editor: A
P-Editor: Zhao S

REFERENCES

1 **Chalasani N**, Younossi Z, Lavine JE, Charlton M, Cusi K, Rinella M, Harrison SA, Brunt EM, Sanyal AJ. The diagnosis and management of nonalcoholic fatty liver disease: Practice guidance from the American Association for the Study of Liver Diseases. *Hepatology* 2018; **67**: 328-357 [PMID: 28714183 DOI: 10.1002/hep.29367]
2 **Younossi ZM**, Koenig AB, Abdelatif D, Fazel Y, Henry L, Wymer M. Global epidemiology of nonalcoholic fatty liver disease-Meta-analytic assessment of prevalence, incidence, and outcomes. *Hepatology* 2016; **64**: 73-84 [PMID: 26707365 DOI: 10.1002/hep.28431]
3 **Wong VW**, Wong GL, Choi PC, Chan AW, Li MK, Chan HY, Chim AM, Yu J, Sung JJ, Chan HL. Disease progression of non-alcoholic fatty liver disease: a prospective study with paired liver biopsies at 3 years. *Gut* 2010; **59**: 969-974 [PMID: 20581244 DOI: 10.1136/gut.2009.205088]
4 **Wong RJ**, Aguilar M, Cheung R, Perumpail RB, Harrison SA, Younossi ZM, Ahmed A. Nonalcoholic steatohepatitis is the second leading etiology of liver disease among adults awaiting liver transplantation in the United States. *Gastroenterology* 2015; **148**: 547-555 [PMID: 25461851 DOI: 10.1053/j.gastro.2014.11.039]
5 **Charlton MR**, Burns JM, Pedersen RA, Watt KD, Heimbach JK, Dierkhising RA. Frequency and outcomes of liver transplantation for nonalcoholic steatohepatitis in the United States. *Gastroenterology* 2011; **141**: 1249-1253 [PMID: 21726509 DOI: 10.1053/j.gastro.2011.06.061]
6 **Byrne CD**, Targher G. NAFLD: a multisystem disease. *J Hepatol* 2015; **62**: S47-S64 [PMID: 25920090 DOI: 10.1016/j.jhep.2014.12.012]
7 **Polyzos SA**, Kountouras J, Mantzoros CS. Obesity and nonalcoholic fatty liver disease: From pathophysiology to therapeutics. *Metabolism* 2019; **92**: 82-97 [PMID: 30502373 DOI: 10.1016/j.metabol.2018.11.014]
8 **Crewe C**, Scherer PE. Intercellular and interorgan crosstalk through adipocyte extracellular vesicles. *Rev Endocr Metab Disord* 2022; **23**: 61-69 [PMID: 33447986 DOI: 10.1007/s11154-020-09625-x]
9 **Ying W**, Riopel M, Bandyopadhyay G, Dong Y, Birmingham A, Seo JB, Ofrecio JM, Wollam J, Hernandez-Carretero A, Fu W, Li P, Olefsky JM. Adipose Tissue Macrophage-Derived Exosomal miRNAs Can Modulate In Vivo and In Vitro Insulin Sensitivity. *Cell* 2017; **171**: 372-384.e12 [PMID: 28942920 DOI: 10.1016/j.cell.2017.08.035]
10 **Liu T**, Sun YC, Cheng P, Shao HG. Adipose tissue macrophage-derived exosomal miR-29a regulates obesity-associated insulin resistance. *Biochem Biophys Res Commun* 2019; **515**: 352-358 [PMID: 31153636 DOI: 10.1016/j.bbrc.2019.05.113]
11 **Rottiers V**, Näär AM. MicroRNAs in metabolism and metabolic disorders. *Nat Rev Mol Cell Biol* 2012; **13**: 239-250 [PMID: 22436747 DOI: 10.1038/nrm3313]
12 **Trajkovski M**, Hausser J, Soutschek J, Bhat B, Akin A, Zavolan M, Heim MH, Stoffel M. MicroRNAs 103 and 107 regulate insulin sensitivity. *Nature* 2011; **474**: 649-653 [PMID: 21654750 DOI: 10.1038/nature10112]
13 **Recena Aydos L**, Aparecida do Amaral L, Serafim de Souza R, Jacobowski AC, Freitas Dos Santos E, Rodrigues Macedo ML. Nonalcoholic Fatty Liver Disease Induced by High-Fat Diet in C57bl/6 Models. *Nutrients* 2019; **11** [PMID: 31888190 DOI: 10.3390/nu11123067]
14 **Wang L**, Zhang X, Lin ZB, Yang PJ, Xu H, Duan JL, Ruan B, Song P, Liu JJ, Yue ZS, Fang ZQ, Hu H, Liu Z, Huang XL, Yang L, Tian S, Tao KS, Han H, Dou KF. Tripartite motif 16 ameliorates nonalcoholic steatohepatitis by promoting the degradation of phospho-TAK1. *Cell Metab* 2021; **33**: 1372-1388.e7 [PMID: 34146477 DOI: 10.1016/j.cmet.2021.05.019]
15 **Gao J**, Li X, Wang Y, Cao Y, Yao D, Sun L, Qin L, Qiu H, Zhan X. Adipocyte-derived extracellular vesicles modulate appetite and weight through mTOR signalling in the hypothalamus. *Acta Physiol (Oxf)* 2020; **228**: e13339 [PMID: 31278836 DOI: 10.1111/apha.13339]
16 **Agarwal V**, Bell GW, Nam JW, Bartel DP. Predicting effective microRNA target sites in mammalian mRNAs. *Elife* 2015; **4** [PMID: 26267216 DOI: 10.7554/eLife.05005]
17 **Younossi ZM**, Tampi R, Priyadarshini M, Nader F, Younossi IM, Racila A. Burden of Illness and Economic Model for Patients With Nonalcoholic Steatohepatitis in the United States. *Hepatology* 2019; **69**: 564-572 [PMID: 30180285 DOI: 10.1002/hep.30254]
18 **Allen AM**, Lazarus JV, Younossi ZM. Healthcare and socioeconomic costs of NAFLD: A global framework to navigate the uncertainties. *J Hepatol* 2023; **79**: 209-217 [PMID: 36740046 DOI: 10.1016/j.jhep.2023.01.026]
19 **Lagos-Quintana M**, Rauhut R, Lendeckel W, Tuschl T. Identification of novel genes coding for small expressed RNAs. *Science* 2001; **294**: 853-858 [PMID: 11679670 DOI: 10.1126/science.1064921]
20 **Voinnet O**. Origin, biogenesis, and activity of plant microRNAs. *Cell* 2009; **136**: 669-687 [PMID: 19239888 DOI: 10.1016/j.cell.2009.01.046]
21 **Vienberg S**, Geiger J, Madsen S, Dalgaard LT. MicroRNAs in metabolism. *Acta Physiol (Oxf)* 2017; **219**: 346-361 [PMID: 27009502 DOI: 10.1111/apha.12681]
22 **Pullen TJ**, da Silva Xavier G, Kelsey G, Rutter GA. miR-29a and miR-29b contribute to pancreatic beta-cell-specific silencing of monocarboxylate transporter 1 (Mct1). *Mol Cell Biol* 2011; **31**: 3182-3194 [PMID: 21646425 DOI: 10.1128/MCB.01433-10]
23 **Belgardt BF**, Ahmed K, Spranger M, Latreille M, Denzler R, Kondratiuk N, von Meyenn F, Villena FN, Herrmanns K, Bosco D, Kerr-Conte J, Pattou F, Rülicke T, Stoffel M. The microRNA-200 family regulates pancreatic beta cell survival in type 2 diabetes. *Nat Med* 2015; **21**: 619-627 [PMID: 25985365 DOI: 10.1038/nm.3862]
24 **Dávalos A**, Goedeke L, Smibert P, Ramírez CM, Warrier NP, Andreo U, Cirera-Salinas D, Rayner K, Suresh U, Pastor-Pareja JC, Esplugues E, Fisher EA, Penalva LO, Moore KJ, Suárez Y, Lai EC, Fernández-Hernando C. miR-33a/b contribute to the regulation of fatty acid metabolism and insulin signaling. *Proc Natl Acad Sci U S A* 2011; **108**: 9232-9237 [PMID: 21576456 DOI: 10.1073/pnas.1102281108]
25 **Rayner KJ**, Esau CC, Hussain FN, McDaniel AL, Marshall SM, van Gils JM, Ray TD, Sheedy FJ, Goedeke L, Liu X, Khatsenko OG, Kaimal V, Lees CJ, Fernandez-Hernando C, Fisher EA, Temel RE, Moore KJ. Inhibition of miR-33a/b in non-human primates raises plasma HDL and lowers VLDL triglycerides. *Nature* 2011; **478**: 404-407 [PMID: 22012398 DOI: 10.1038/nature10486]
26 **Krützfeldt J**, Rajewsky N, Braich R, Rajeev KG, Tuschl T, Manoharan M, Stoffel M. Silencing of microRNAs *in vivo* with 'antagomirs'. *Nature* 2005; **438**: 685-689 [PMID: 16258535 DOI: 10.1038/nature04303]

27 **Esau C**, Davis S, Murray SF, Yu XX, Pandey SK, Pear M, Watts L, Booten SL, Graham M, McKay R, Subramaniam A, Propp S, Lollo BA, Freier S, Bennett CF, Bhanot S, Monia BP. miR-122 regulation of lipid metabolism revealed by *in vivo* antisense targeting. *Cell Metab* 2006; **3**: 87-98 [PMID: 16459310 DOI: 10.1016/j.cmet.2006.01.005]

28 **DiStefano JK**. NAFLD and NASH in Postmenopausal Women: Implications for Diagnosis and Treatment. *Endocrinology* 2020; **161** [PMID: 32776116 DOI: 10.1210/endocr/bqaa134]

29 **Fang T**, Li J, Wu X. Shenmai injection improves the postoperative immune function of papillary thyroid carcinoma patients by inhibiting differentiation into Treg cells *via* miR-103/GPER1 axis. *Drug Dev Res* 2018; **79**: 324-331 [PMID: 30267584 DOI: 10.1002/ddr.21459]

30 **Thietart S**, Rautou PE. Extracellular vesicles as biomarkers in liver diseases: A clinician's point of view. *J Hepatol* 2020; **73**: 1507-1525 [PMID: 32682050 DOI: 10.1016/j.jhep.2020.07.014]

31 **Fuchs A**, Samovski D, Smith GI, Cifarelli V, Farabi SS, Yoshino J, Pietka T, Chang SW, Ghosh S, Myckatyn TM, Klein S. Associations Among Adipose Tissue Immunology, Inflammation, Exosomes and Insulin Sensitivity in People With Obesity and Nonalcoholic Fatty Liver Disease. *Gastroenterology* 2021; **161**: 968-981.e12 [PMID: 34004161 DOI: 10.1053/j.gastro.2021.05.008]

32 **Klionsky DJ**, Emr SD. Autophagy as a regulated pathway of cellular degradation. *Science* 2000; **290**: 1717-1721 [PMID: 11099404 DOI: 10.1126/science.290.5497.1717]

33 **Mizushima N**, Levine B, Cuervo AM, Klionsky DJ. Autophagy fights disease through cellular self-digestion. *Nature* 2008; **451**: 1069-1075 [PMID: 18305538 DOI: 10.1038/nature06639]

34 **Ueno T**, Komatsu M. Autophagy in the liver: functions in health and disease. *Nat Rev Gastroenterol Hepatol* 2017; **14**: 170-184 [PMID: 28053338 DOI: 10.1038/nrgastro.2016.185]

35 **Jin X**, Gao J, Zheng R, Yu M, Ren Y, Yan T, Huang Y, Li Y. Antagonizing circRNA_002581-miR-122-CPEB1 axis alleviates NASH through restoring PTEN-AMPK-mTOR pathway regulated autophagy. *Cell Death Dis* 2020; **11**: 123 [PMID: 32054840 DOI: 10.1038/s41419-020-2293-7]

36 **Qian H**, Chao X, Williams J, Fulte S, Li T, Yang L, Ding WX. Autophagy in liver diseases: A review. *Mol Aspects Med* 2021; **82**: 100973 [PMID: 34120768 DOI: 10.1016/j.mam.2021.100973]

37 **Zhou J**, Tripathi M, Ho JP, Widjaja AA, Shekeran SG, Camat MD, James A, Wu Y, Ching J, Kovalik JP, Lim KH, Cook SA, Bay BH, Singh BK, Yen PM. Thyroid Hormone Decreases Hepatic Steatosis, Inflammation, and Fibrosis in a Dietary Mouse Model of Nonalcoholic Steatohepatitis. *Thyroid* 2022; **32**: 725-738 [PMID: 35317606 DOI: 10.1089/thy.2021.0621]

38 **Sinha RA**, Farah BL, Singh BK, Siddique MM, Li Y, Wu Y, Ilkayeva OR, Gooding J, Ching J, Zhou J, Martinez L, Xie S, Bay BH, Summers SA, Newgard CB, Yen PM. Caffeine stimulates hepatic lipid metabolism by the autophagy-lysosomal pathway in mice. *Hepatology* 2014; **59**: 1366-1380 [PMID: 23929677 DOI: 10.1002/hep.26667]

Published by **Baishideng Publishing Group Inc**
7041 Koll Center Parkway, Suite 160, Pleasanton, CA 94566, USA
Telephone: +1-925-3991568
E-mail: bpgoffice@wjgnet.com
Help Desk: https://www.f6publishing.com/helpdesk
https://www.wjgnet.com